Biochimica et Biophysica Acta 1807 (2011) 205–215

Contents lists available at ScienceDirect

Biochimica et Biophysica Acta

journal homepage: www.elsevier.com/locate/bbabio

Electron paramagnetic resonance study of the electron transfer reactions in photosystem II membrane preparations from *Arabidopsis thaliana*

Guiying Chen [a], Yagut Allahverdiyeva [b], Eva-Mari Aro [b], Stenbjörn Styring [a], Fikret Mamedov [a,*]

[a] Department of Photochemistry and Molecular Science, Ångström Laboratory, Box 523, Uppsala University, SE-751 20 Uppsala, Sweden
[b] Department of Biochemistry and Food Chemistry, Plant Physiology and Molecular Biology, University of Turku, FI-20014 Turku, Finland

ARTICLE INFO

Article history:
Received 1 August 2010
Received in revised form 6 October 2010
Accepted 8 October 2010
Available online 15 October 2010

Keywords:
Photosystem II
Electron paramagnetic resonance
Arabidopsis thaliana

ABSTRACT

Arabidopsis thaliana is widely used as a model organism in plant biology as its genome has been sequenced and transformation is known to be efficient. A large number of mutant lines and genomic resources are available for *Arabidopsis*. All this makes *Arabidopsis* a useful tool for studies of photosynthetic reactions in higher plants. In this study, photosystem II (PSII) enriched membranes were successfully isolated from thylakoids of *Arabidopsis* plants and for the first time the electron transfer cofactors in PSII were systematically studied using electron paramagnetic resonance (EPR) spectroscopy. EPR signals from both of the donor and acceptor sides of PSII, as well as from auxiliary electron donors were recorded. From the acceptor side of PSII, EPR signals from Q_A^- Fe^{2+} and Phe^- Q_A^- Fe^{2+} as well as from the free Phe^- radical were observed. The multiline EPR signals from the S_0- and S_2-states of $CaMn_4O_x$-cluster in the water oxidation complex were characterized. Moreover, split EPR signals, the interaction signals from $Y_Z^\bullet$ and $CaMn_4O_x$-cluster in the S_0-, S_1-, S_2-, and the S_3-state were induced by illumination of the PSII membranes at 5 K and characterized. In addition, EPR signals from auxiliary donors $Y_D^\bullet$, Chl^+ and cytochrome b_{559} were observed. In total, we were able to detect about 20 different EPR signals covering all electron transfer components in PSII. Use of this spectroscopic platform opens a possibility to study PSII reactions in the library of mutants available in *Arabidopsis*.

1. Introduction

Higher plants are widely spread over terrestrial ecosystems and exhibit a high degree of diversity, which enables them to grow under very different environmental conditions. One of the reasons for such plasticity is that plants possess the most efficient and dynamic photosynthetic apparatus. Their photosynthetic machinery is situated in chloroplasts and the light harvesting and energy transduction systems are embedded into highly organized membrane structures.

Arabidopsis thaliana (hereafter *Arabidopsis*) is a small flowering plant with a modest genome size which has been sequenced in the year 2000 [1]. Since then *Arabidopsis* has been widely used as a model organism in plant biology for the following reasons: (i) it has a rapid life cycle (about 6 weeks from germination to mature seed); (ii) extensive genetic and physical maps of all 5 chromosomes of *Arabidopsis* are available; (iii) efficient transformation methods have been developed and (iv) a large number of mutant lines and genomic resources are available from Stock Centers [2–4]. All this makes *Arabidopsis* an important object also for studies of the primary photosynthetic reactions in higher plants.

In recent years, the use *Arabidopsis* mutants for detailed analysis of the photosynthetic apparatus in the thylakoid membrane has increased. This approach has been pivotal for studies focusing on regulation of light harvesting [5–7], linear and cyclic electron flow [8–12], the structure and function of photosystem I (PSI)[1], Cyt b_6f and NDH-complexes [8,10–14], oxidative, temperature stress and photoinhibition [15–18], chloroplast development and biogenesis of the photosynthetic complexes [19,20], the redox signaling in chloroplasts [19], etc.

This also holds for studies of structure and function of PSII. PSII is a large multiprotein–pigment complex which in its active form in higher plants is mostly found in the stacked granal membranes of chloroplasts [21–23]. It initiates the photosynthetic electron flow by using light energy to extract electrons from water and to reduce the pool of the plastoquinone molecules [24,25]. About ten redox active cofactors, mostly bound to the D1/D2 protein heterodimer participate in this reaction. The $CaMn_4O_x$-cluster and the redox active tyrosine

Abbreviations: Car, carotenoid; Chl, chlorophyll; Cyt b_{559}, cytochrome b_{559}; DCIP, 2,6-dichlorophenolindophenol; DPC, 2,2′-diphenylcarbonic dihydrazide; EPR, electron paramagnetic resonance; HP and LP, high and low potential forms of oxidized Cyt b_{559}; MA, modulation amplitude; NIR, near infrared; RT, room temperature; P680, primary electron donor chlorophylls in PSII; P*p*BQ, phenyl-*p*-benzoquinone; PSII, photosystem II; Phe, pheophytin, acceptor of PSII; Q_A and Q_B, primary and secondary quinine acceptors of PSII; S states, intermediates in the cyclic turnover of the WOC; WOC, water oxidation complex; WT, wild type; Y_D and $Y_D^\bullet$, tyrosine 161 of the D2 polypeptide of PSII and its radical; Y_Z and $Y_Z^\bullet$, tyrosine 161 of the D1 polypeptide of PSII and its radical

* Corresponding author. Tel.: +46 18 471 6581; fax: +46 471 6844.
E-mail address: fikret.mamedov@fotomol.uu.se (F. Mamedov).

0005-2728/$ – see front matter © 2010 Elsevier B.V. All rights reserved.
doi:10.1016/j.bbabio.2010.10.010

residue, Y_Z, constitute the catalytic site — WOC, where the water oxidation takes place [26–30]. P_{680} is the primary electron donor in PSII and is composed of a tetramer of Chls. After excitation from antenna Chls, P_{680} transfers an electron to the acceptor side of PSII. P_{680}^{+} is strongly oxidizing and extracts electrons from the WOC which circulates through the five intermediate states, denoted $S_0 \rightarrow S_4$ [26,27,30,31]. After excitation, electrons from P_{680} first reduce the Phe and subsequently Q_A and Q_B, the primary and secondary quinone acceptors in PSII. After accepting two electrons and two protons, Q_B leaves PSII in the plastoquinol form.

The many redox components in PSII can be studied by a diversity of spectroscopic methods. One of the few techniques that give access to nearly all of the redox components, including the WOC in all S states, is EPR spectroscopy. With EPR spectroscopy both the structure and the function of the redox center can be studied, often in molecular details. In PSII research EPR has been applied also to studies of the effects of many site-directed mutants on for example the $CaMn_4O_x$-cluster. Most EPR work applied to mutants has been performed in cyanobacteria and algae but there also valuable EPR studies in naturally occurring mutants in plants. This does not hold for *Arabidopsis* and there are very few EPR studies in this plant despite its huge genetic importance.

The wild type and mutants in PSII subunits of *Arabidopsis* have been widely used in studies of the protein composition of PSII [32–38], electron transfer reactions and the mechanism of water oxidation [33,35,38]. However, these experiments were mostly performed in intact leaves or isolated thylakoid membranes. In this study, we have used highly active PSII enriched membranes isolated from thylakoids of *Arabidopsis* plants [38] to perform a systematic characterization with EPR spectroscopy of the electron transfer cofactors in PSII and intermediates in the water oxidation process. Our study describes nearly 20 different EPR signals representing all redox components in PSII. Thus, presented results provide the first strong spectroscopic platform for PSII studies in *Arabidopsis* and extend the molecular studies of PSII to another higher plant species.

2. Materials and methods

2.1. Plant material and isolation of PSII-enriched membranes

Arabidopsis plants (ecotype Columbia) were grown on soil under standard growth chamber conditions (23 °C, 120 μmol photons m^{-2} s^{-1}, a light/dark cycle 8/16 h) for 7 weeks. PSII-enriched membranes (BBY-type) were isolated from mature plant leaves according to the procedure of Berthold et al. [39] with some modifications. Leaves were ground in ice-cold buffer containing 20 mM Tricine/NaOH (pH 8.4), 0.45 M sorbitol, 10 mM Na-EDTA, 5 mM NaCl, 5 mM $MgCl_2$ and freshly added 0.2% BSA and 0.2% Na-ascorbate. The homogenate was filtered through Miracloth and centrifuged at 4200×*g* for 10 min at 4 °C. The pellet was washed with 20 mM Tricine/NaOH (pH 7.6), 0.33 M sorbitol, 5 mM $MgCl_2$ and re-suspended in a buffer containing 20 mM Tricine/NaOH (pH 7.6) and 5 mM $MgCl_2$. After centrifugation at 4200×*g*, the pellet was re-suspended in 20 mM MES/NaOH (pH 6.3), 5 mM $MgCl_2$ and 15 mM NaCl. After the Chl concentration was adjusted to 2.67 mg/ml, 1/3 volume of 20% Triton X-100 was added slowly to the sample suspension and stirred for 30 min on ice in darkness. The sample was then centrifuged at 9300×*g* for 3 min and the supernatant again at 42 000×*g* for 30 min. The pellet was re-suspended in the same buffer without Triton and again centrifuged at 42 000×*g* for 30 min. Finally, the pellet was suspended in buffer containing 20 mM Mes/NaOH (pH 6.3), 0.4 M sorbitol, 15 mM NaCl, 10 mM $CaCl_2$ and 5 mM $MgCl_2$. The Chl concentration was measured according to Porra et al. [40].

2.2. Analysis of the protein composition and general characterization

Polypeptides were separated with SDS-PAGE (15% polyacrilamide, 6 M urea) [41]. After electrophoresis polypeptides were stained with Coomassie Blue or electroblotted to a polyvinylidenefluoride membrane and immunodetected with specific antibodies. Oxygen evolution and variable fluorescence were measured as in [34]. The number of active PSII centers was determined by measuring DCIP reduction in the absence and presence exogenous electron donor DPC as described in [21]. The PSI/PSII ratio was determined by EPR measurements at room temperature as in [42].

2.2.1. EPR samples preparation

PSII enriched membranes were diluted to 2 mg Chl/ml and filled into calibrated EPR tubes. For quantification of Y_D•, the sample was exposed to room light for 3 min to fully oxidize Y_D and thereafter dark incubated for 15 min at room temperature before freezing or application of the pre-flash protocol [43]. All spectra obtained at this point are considered as EPR spectra of dark-adapted samples.

2.2.2. Synchronization of the WOC in the S_1-state

PSII in the samples with fully oxidized Y_D were synchronized to contain an absolute majority of the dark stable S_1-state by the application of two saturating pre-flashes from a Nd:YAG laser from Spectra Physics, Newport, USA (532 nm, 450 mJ, 6 ns, 1.25 Hz) followed by dark adaptation for 20 min at room temperature [43–46].

2.2.3. Flash-induced turnover of the WOC

To study EPR signals from PSII in the different S states, the synchronized samples were advanced to the other S states by giving a corresponding number of saturating laser flashes [44]. Before the flashes, P*p*BQ was added as an external electron acceptor to a final concentration of 0.5 mM (from a stock solution in DMSO or methanol, final solvent concentration 3% v/v) in darkness at room temperature. 30 s after the addition of P*p*BQ, the samples were transferred to an ethanol bath at 1 °C and allowed to equilibrate for 1 min. After the equilibration, the samples were transferred to the flash cell and were immediately given one, two or three turnover flashes (532 nm, 450 mJ, 6 ns, 1.25 Hz). After flashes, the EPR samples were immediately frozen in an ethanol-dry ice bath (198 K) within 1–2 s and flushed with argon gas before being transferred to liquid nitrogen for EPR measurements.

2.2.4. Induction of EPR signals from the acceptor side of PSII

To chemically induce the Q_A^- Fe^{2+} interaction signal, EPR samples were incubated for 15 min after the addition of 50 mM Na-formate followed by addition with 50 mM Na-dithionite and a second incubation for 10 min in the darkness at room temperature [47–50]. To induce the split Phe^- signal (the Phe^- Q_A^- Fe^{2+} interaction signal) the formate and dithionite treated samples were illuminated at 198 K for 10 min [48,51]. The Phe^- radical signal was photo-accumulated in the formate and dithionite treated samples by illumination at room temperature for 10 min [47,52].

To photo-induce the spin-polarized triplet $^3P_{680}$ EPR signal, PSII samples were incubated at anaerobic conditions with 50 mM Na-dithionite and 30 μM benzyl viologen at room temperature for 1 h [53]. The signal was generated by direct illumination into the EPR cavity.

2.2.5. Illumination conditions

The S_2-state multiline EPR signal was in some cases also induced by illumination for 6 min at 198 K in an ethanol-dry ice bath. Complete oxidation of Cyt b_{559} was achieved by illumination for 6 min at 77 K. White light from a halogen lamp (800 W) filtered with a 5 cm thick $CuSO_4$ solution was used in both cases.

2.2.6. Induction of split EPR signals from the WOC

The split EPR signals from the S_1, S_2, S_3 and the S_0-states were induced by direct illumination of samples in the EPR cavity as described in [54]. The Split S_1, Split S_2 (in the presence of methanol) and Split S_0 signals were induced with illumination by visible light for 30 s at 5 K. The light was filtered through a 5 cm thick $CuSO_4$ solution and directed into the EPR cavity using a transparent Plexiglas light guide. The intensity measured at the position of the resonator window was 450 W/m^2. The Split S_3 EPR signal was induced by either visible or by NIR illumination at 830 nm for 20 min at 5 K (LQC830-135E laser diode, Newport, USA), with a beam-spreader lens placed in front of the EPR cavity window. The NIR light intensity at the EPR resonator window was 280 W/m^2. The Split S_2 EPR signal in the absence of methanol was induced according to [55] in the following way. First, the temperature in the resonator with the sample was raised to about 200 K and illumination with visible light was applied. Subsequently, the temperature was decreased to 5 K during illumination and the spectrum of the Split S_2 signal was recorded.

2.3. EPR measurements

Continuous-wave X-band EPR measurements were performed with a Bruker ELEXYS E500 spectrometer using a SuperX EPR049 microwave bridge and a SHQ4122 resonator. The system was fitted with an ESR 900 liquid helium cryostat and ITC 503 temperature controller (Oxford Instruments Ltd., UK). EPR settings are given in the corresponding figure legends. Signal processing and analysis were carried out with the Bruker Xepr software. EPR signals were corrected for variations in the sample volume and Chl concentration using the non-saturated EPR signal from Y_D• as described in [43,56], when it was necessary for comparison.

3. Results and discussion

3.1. Preparation and characterization of the PSII membranes from Arabidopsis

Thylakoid membrane preparations from *Arabidopsis* have been described and used for characterization of the PSII properties [38]. In the preparation of the PSII enriched membranes the well-known protocol from Bethold, Babcock and Yocum, developed for spinach, was used as a basis [39]. However, some modifications, like a higher pH and a high amount of Na-Asc and BSA in the grinding buffer to inhibit myrosinase and to neutralize proteases, were necessary for obtaining active PSII membrane preparations from *Arabidopsis*.

Protein composition of the obtained PSII membranes is shown in Fig. 1. SDS-PAGE in the presence of 6 M urea revealed the presence of the major PSII protein subunits visible after Coomassie staining: CP47, CP43, LHCII and three extrinsic subunits PsbO, PsbP and PsbQ. It also shows that proteins associated with other complexes such as ATP-synthase are absent in our preparation (Fig. 1A). Furthermore, the absence of PSI proteins was confirmed by immunoblot analysis — PsaB, the core subunit of PSI, was not detected in our preparation of PSII membranes (Fig. 1B).

Some characterization of the PSII membranes from *Arabidopsis* is shown in Table 1. The quality of the PSII membrane preparation is affirmed by the low Chl *a*/*b* ratio which is similar to ratio in for example preparations from spinach or pea. Increased oxygen evolution rates and variable fluorescence (F_V/F_M ratio, [57]) were observed in the PSII membranes if compared to thylakoid preparations. The increases are not very large. This could reflect a partially damaged WOC in the PSII membrane preparation. This was tested by measurements of DCIP reduction in the presence and absence of the electron donor DPC which showed that <5% of PSII centers in our preparation were inactive in oxygen evolution (not shown). Instead we attribute unexpectedly low oxygen evolution to a modified Q_B site, which is common to PSII in purified preparations. Importantly, the contamination from the remaining PSI centers on the basis of EPR measurements (much more sensitive if compared to the protein analysis, [42]) was found to be <10%, which is important for the spectroscopic characterization of PSII.

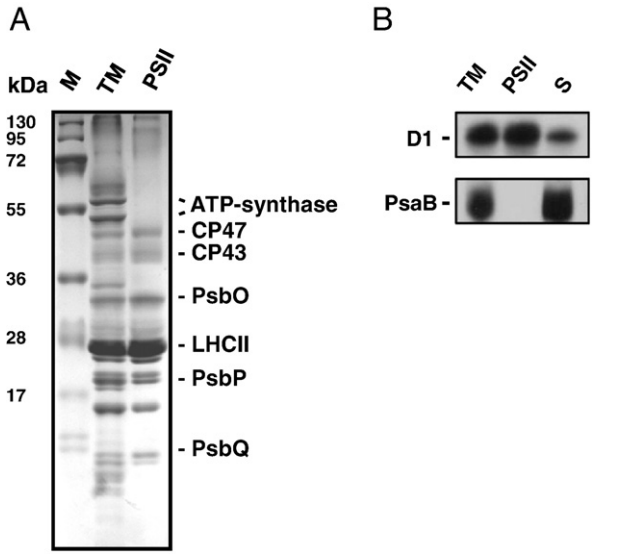

Fig. 1. Protein profiles of the thylakoid membrane and the PSII enriched membranes isolated from *Arabidopsis*. A — Coomassie Blue-stained gel demonstrating markers (M), the thylakoid membrane (TM) and the PSII enriched membrane (PSII). B — analysis of the PSII and PSI content of the thylakoid membrane (TM), PSII enriched membranes (PSII) and supernatant obtained after Triton-treatment (S). Samples were subjected to SDS-PAGE electrophoresis in the presence of 6 M urea, followed by immunoblotting with antibodies against D1 protein of PSII complex and PsaB protein of PSI complex. Gels were loaded on the Chl basis.

3.1.1. EPR signals originating from the acceptor side of PSII

The EPR signals associated with the acceptor side of PSII from *Arabidopsis* are shown in Fig. 2 (see also Table 2 for a compilation of all EPR signals). It is known that the reduced primary acceptor, Q_A^-, is a semiquinone anion radical which magnetically interacts with a nearby Fe^{2+} ion. PSII membranes from other organisms (cyanobacteria, green algae and spinach) show two types of EPR signals at $g = 1.90$ and 1.64, or at $g = 1.82$ and 1.67, depending on the signal induction conditions [47,58,59]. These signals are usually not easily observed in the EPR spectra. Addition of Na-formate to the PSII membranes isolated from spinach (and some other species) has been found to greatly increase the amplitude of the $g = 1.82$ form with concomitant decrease in $g = 1.90$ form [48]. The EPR signal from $Q_A^-Fe^{2+}$ complex obtained in the presence of formate and dithionite from PSII enriched membranes of *Arabidopsis* is depicted in Fig. 2A. It shows a peak at $g = 1.84$ and a broad minimum at $g = 1.73$ with full width of 230 G (Table 2) and is similar to the spectra reported from spinach [23,47] and cyanobacterial preparations [58,60].

The non-heme iron is located between the electron acceptors, Q_A and Q_B, in PSII [61]. The high spin Fe^{2+} can be oxidized to Fe^{3+} by some external oxidants such as P*p*BQ$^-$•, giving rise to broad EPR features in the $g = 5$–8 region [62–64]. The corresponding signals

Table 1
General characteristics of the PSII membrane preparation from *Arabidopsis*.

	O_2 evolution	F_V/F_M	PSI/PSII ratio	Chl *a*/*b* ratio
Thylakoids	333 ± 18	0.73	0.91	3.2
PSII membranes	399 ± 17	0.78	0.09	2.1

The oxygen evolution is given in μmol of O_2 per mg of Chl per h and was measured in 50 mM HEPES/KOH (pH 7.5), 0.1 M sorbitol, 10 mM $MgCl_2$ and 2.5 mM $CaCl_2$ (thylakoids) or 20 mM MES/NaOH (pH6.3), 0.4 M sorbitol, 5 mM $MgCl_2$, 15 mM NaCl, and 2.5 mM $CaCl_2$ (PSII membranes). The PSI/PSII ratio was determined as described in [42].

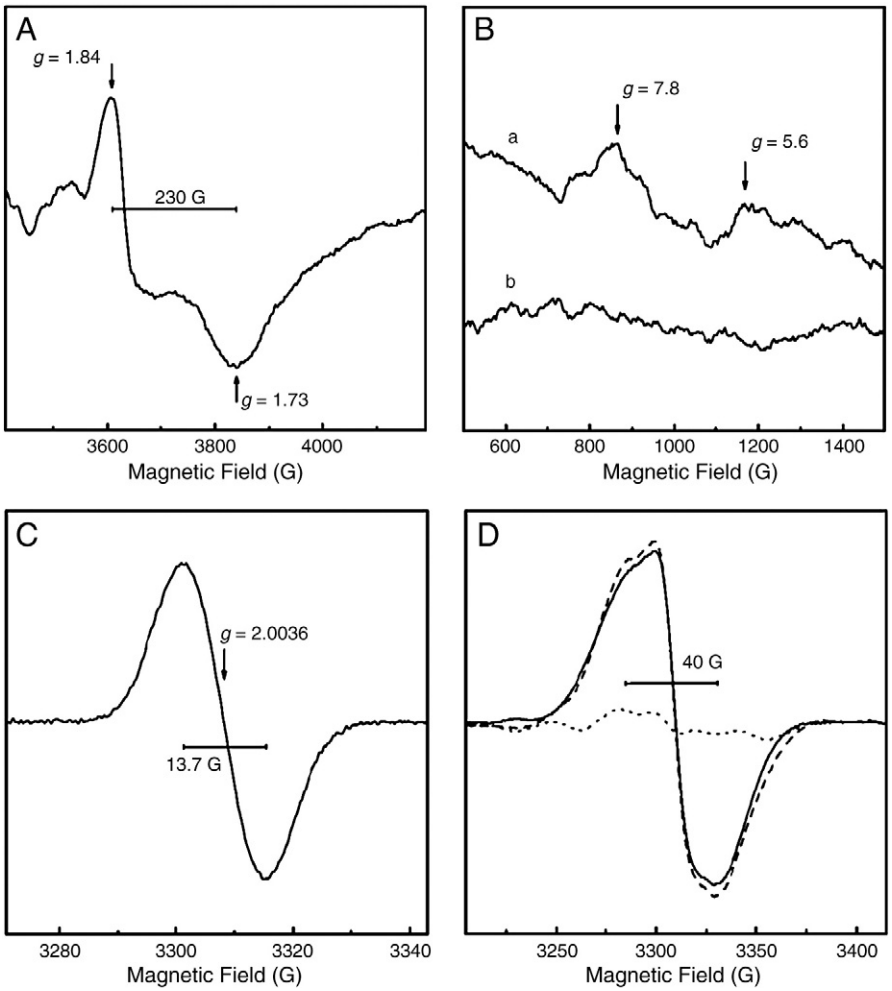

Fig. 2. EPR characterization of the acceptor side of PSII in *Arabidopsis*. (A) EPR spectrum from the primary semiquinone–iron (Q_A^- Fe^{2+}) complex after incubation of PSII enriched membranes in the presence of 50 mM Na-formate and 50 mM Na-dithionite. EPR conditions: microwave power 25 mW, microwave frequency 9.275 GHz, modulation amplitude 20 G, temperature, 4.4 K. (B) Light minus dark difference EPR spectra obtained after a saturating laser flash in the presence of 0.5 mM P*p*BQ (spectrum a) or continuous illumination at 200 K for 8 min (spectrum b). Spectrum a shows two signals from the oxidized non-heme iron in PSII. EPR settings: microwave power 10 mW, microwave frequency 9.275 GHz, modulation amplitude 20 G, temperature 7 K. (C) EPR spectrum from Phe radical after chemical reduction as in A followed by illumination at 295 K for 10 min. EPR conditions: microwave power 1.3 μW, microwave frequency 9.275 GHz, modulation amplitude 3.5 G, temperature 15 K. (D) Photoinduction of the Phe^- Q_A^- Fe^{2+} interaction EPR signal after chemical reduction as in (A). The spectra shown are taken before illumination (dotted line), after illumination at 200 K for 10 min (dashed line) and as light minus dark difference (solid line). EPR conditions: microwave power 25 mW, microwave frequency 9.275 GHz, modulation amplitude 10 G, temperature, 4.4 K.

from *Arabidopsis* are presented in Fig. 2B and show two peaks at $g = 5.6$ and $g = 7.8$ in the presence of P*p*BQ (Fig. 2B, spectrum a, Table 2). The two peaks were suggested to originate from the ground state and the first excited state of high spin non-heme Fe^{3+} respectively [65]. Apparently, these peaks are not detectable in the absence of artificial electron acceptor (spectrum b). Our observation here implies that the oxidation of the non-heme iron by the semi-reduced external acceptor $PpBQ^-$ [62,66] also occurs in PSII enriched membranes of *Arabidopsis*.

If the primary quinone acceptor, Q_A, can be overreduced to the abnormal double reduced diamagnetic Q_AH_2 state, continued illumination can allow the observation of the reduced intermediate electron acceptor in PSII, Phe^-. In PSII samples reduced with dithionite, further illumination at room temperature forces the double reduction of Q_A^- and enables accumulation of the Phe^- radical [51,52,67,68]. The EPR spectrum from Phe^- obtained after reduction of the samples with Na-dithionate and illumination for 10 min (photoaccumulation) at room temperature is depicted in Fig. 2C. The EPR signal obtained from the PSII enriched membranes of *Arabidopsis* is centered at $g = 2.0036$ and exhibits a symmetrical single line with a $\Delta H = 13.7$ G from peak to trough (Table 2). It was noted that Y_D is completely reduced by the addition of 50 mM Na-dithionite as no $Y_D^\bullet$ was detected in the spectra before illumination (not shown). Illumination of samples for 10 min induced 80 % of Phe^- (on the basis of the $Y_D^\bullet$ signal present before dithionite addition) which is comparable to the maximal induction level in similar preparations from other species [49,68].

When illumination in the presence of formate and dithionite was done at 200 K instead of room temperature, the primary quinone acceptor stayed single reduced and accumulation of the Phe radical leads to a complex interaction signal involving Q_A^-, Fe^{2+} and Phe^- [51,59]. This so called split Phe^- EPR signal, originating from the Phe^- radical and being broadened by the presence of the nearby Q_A^- Fe^{2+} in PSII from *Arabidopsis*, is shown in Fig. 1D. Before illumination, no split Phe^- signal was detected around the $g = 2$ region (dotted line). 200 K illumination induced a signal (Fig. 2D, dashed line) which is also shown as a light minus dark difference spectrum (Fig. 2D, solid line). The EPR spectrum obtained from PSII enriched membranes of *Arabidopsis* is different from, but resembles, the split Phe^- signal reported from spinach [49,51,59]. It is known that the splitting depends on the type of the Q_A^- Fe^{2+} signal that is present [59]. The presence of formate in our samples, and therefore the dominance of the $g = 1.84$ form of the Q_A^- Fe^{2+} signal (Fig. 2A), lead to the 40 G wide

Table 2
Summary of EPR signals recorded in PSII membranes from *Arabidopsis*. Only the EPR signals induction conditions used in this study are listed. All signals are recorded with X-band perpendicular mode EPR[a].

Signal identity	Spectral features	Measuring conditions	Induction conditions	Refs.[b]
Acceptor side of PSII				
Phe^- primary acceptor	$g=2.0036$, 13.7 G wide	15 K, 1.3 μW, 3.5 G MA	Light at RT, chemical reduction (50 mM dithionite)	Fig. 2C, [52]
Q_A^- Fe^{2+} Phe^- interaction signal	$g\sim2$, ~40 G wide	4–5 K, 25 mW, 10 G MA	Light at 200 K, chemical reduction (50 mM dithionite and 50 mM formate)	Fig. 2D, [51]
Q_A^- Fe^{2+} interaction signal	$g=1.84$ peak, $g=1.73$ trough 230 G wide	4–5 K, 25 mW, 10 G MA	RT, chemical reduction (50 mM dithionite and 50 mM formate)	Fig. 2A, [58,59]
Fe^{3+} signal	$g=5.6$ and 7.8 peaks	7 K, 10 mW, 20 G MA	Light at RT, 0.5 mM P*p*BQ	Fig. 2B, [62]
Donor side of PSII — primary and auxiliary donors				
$^3P_{680}$, triplet state of the primary donor	$g\sim2$ >600 G wide	4–5 K, 63 μW, 20 G MA	Light at 4–5 K, chemical reduction (50 mM dithionite and 30 μM benzyl viologen)	Fig. 3, [69,71]
$Y_D^\bullet$ tyrosine radical, auxiliary donor	$g=2.0046$, 19 G wide	15 K, 1.3 μW, 3.5 G MA	Light at RT, very stable	Fig. 4A, [79,80]
Chl_Z^+, Car^+ auxiliary donors	$g=2.0026$, 9–10 G wide	15 K, 1.3 μW, 3.5 G MA	Light at ≤200 K	Fig. 4A, [81]
Cyt b_{559} auxiliary donor/acceptor	$g_z=2.9$–3.1, $g_y=2.2$–2.1, $g_z=1.43$ (hardly observable)	15 K, 5 mW, 15 G MA	Light at ≤77 K	Fig. 4B, [75]
Donor side of PSII — water oxidizing complex				
S_2 state multiline signal	$g\sim2$, ≥18 lines, 80–90 G spacing, >1800 G wide	7 K, 10 mW, 20 G MA	S_2 state, light at RT or 200 K, 0.5 mM P*p*BQ (optional)	Fig. 5, [87,90]
S_2 state $g=4.1$ signal	$g=4.1$, 240 G wide	7 K, 10 mW, 20 G MA	S_2 state, light at 200 K, –MeOH	Fig. 5, [89]
S_0 state multiline signal	$g\sim2$, ≥24 lines, 80–90 G spacing, >2200 G wide	7 K, 20 mW, 20 G MA	S_0 state, light at RT, 0.5 mM P*p*BQ and MeOH	Fig. 5, [45,97]
S_1 state $Y_Z^\bullet$ interaction signal, Split S_1	$g=2.035$ peak, $g\sim2.0$ derivative, asymmetrical	5 K, 20 mW 15 G MA	S_1 state, light at 5 K, 0.5 mM P*p*BQ, –MeOH	Fig. 6A, [101]
S_2 state $Y_Z^\bullet$ interaction signal, Split S_2	$g=2.055$ peak, $g\sim2.0$ derivative, asymmetrical	5 K, 50 mW 15 G MA	S_2 state, light at 200 K and cooling under illumination to 5 K, 0.5 mM P*p*BQ, –MeOH	Fig. 6B, [55]
S_2 state $Y_Z^\bullet$ interaction signal, Split S_2	$g\sim2.0$ derivative, symmetrical, 140 G wide	5 K, 50 mW 15 G MA	S_2 state, light at 5 K, 0.5 mM P*p*BQ, +MeOH	Fig. 6B, [55]
S_3 state $Y_Z^\bullet$ interaction signal, Split S_3	$g=2.06$ peak, $g=1.95$ and 1.93 trough, asymmetrical	5 K, 20 mW 15 G MA	S_3 state, visible or NIR light at 5 K, 0.5 mM P*p*BQ, –MeOH	Fig. 6C, [107,113]
S_0 state $Y_Z^\bullet$ interaction signal, split S_0	$g\sim2.0$ derivative, symmetrical, 165 G wide	5 K, 20 mW 15 G MA	S_0 state, light at 5 K, 0.5 mM P*p*BQ, ±MeOH	Fig. 6D, [101]

[a] So far we have not been able to record successfully EPR signals from Arabidopsis in the parallel mode EPR or with higher frequency EPR. This partly reflects lack of suitable biological material, partly the small size of the signals.
[a] Figure number refers to figure in this work. Reference number refers to EPR spectra obtained in other organisms, plant or cyanobacteria.

splitting of the Phe^- Q_A^- Fe^{2+} split signal in *Arabidopsis* (Fig. 1D, Table 2).

3.1.2. Induction of the spin-polarized triplet $^3P_{680}$ state

The triplet state of the primary electron donor in PSII is formed when samples, in which the quinone-iron acceptor complex is fully reduced or absent, are illuminated at cryogenic temperatures [69,70]. Under these conditions charge separation occurs with the formation of the radical pair, P_{680}^+ Phe^- [71]. The short-lived radical pair decays via a spin-polarized triplet state of P_{680} which is relatively long lived and exhibits a characteristic doublet EPR signal [53,71–73]. Fig. 3 shows the light minus dark difference spectrum of the spin-polarized $^3P_{680}$ EPR signal induced by continuous illumination at 4 K. The dithionite and benzyl viologen reduced PSII enriched membranes from *Arabidopsis* displayed no signal from Q_A^- Fe^{2+} indicating that Q_A was double reduced by dithionite at room temperature forming a protonated Q_AH_2 state which is EPR silent (not shown). This reaction was accelerated by the presence of benzyl viologen [71]. The light spectrum was taken during illumination at 4 K and shows the $^3P_{680}$ signal formation. The signal decays within our time resolution after termination of light. The decay has been reported to occur with a half-time of several microseconds at 4 K in other plant materials [71]. The light minus dark difference spectrum exhibited symmetrical splitting feature of the polarized triplet $^3P_{680}$ EPR signal centered around $g=2$ and

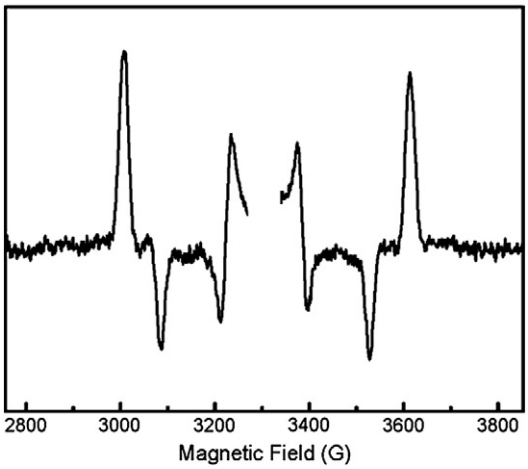

Fig. 3. The light minus dark difference EPR spectrum from the spin-polarized triplet state of ^{3}P680 obtained in the presence of Na-dithionite and benzyl viologen (more details in the Materials and methods section). The light spectrum was acquired under continuous illumination at 4.1 K. EPR conditions: microwave power 63 μW, microwave frequency 9.275 GHz, modulation amplitude 20 G, temperature, 4.1 K.

extended over 600 G (Table 2), similar to those from spinach [53,71,73] and pea preparations [70].

3.2. Auxiliary electron donors in PSII

The primary electron donor source to P_{680}^{+} in PSII is the WOC complex and will be analyzed (with respect to PSII from *Arabidopsis*) in the next section. However, in some cases, when the water splitting activity of PSII is impaired or diminished, other auxiliary, secondary electron donors in PSII come into play. This is a typical situation under stress conditions, when PSII is photoinhibited or during the recovery and photoactivation processes [74]. Illumination of PSII at low and cryogenic temperatures, when the S state transitions in WOC are blocked, also lead to oxidation of auxiliary, secondary donors in PSII [75–78]. These electron donors include Y_D, Chl, Car and Cyt b_{559}. Here we characterized these electron transfer cofactors involved in side-pathways in PSII from *Arabidopsis*.

The Y_D• EPR signal from dark adapted PSII membranes from *Arabidopsis* is shown in Fig. 3A (spectra a, solid line). The signal is centered at $g = 2.0046$, and shows essentially no difference from the Y_D• signal from other species (Table 2) as judged by the line shape and the g value, indicating that Y_D• exists in a very similar protein environment. The Y_D• radical is very stable and corresponds to one spin per PSII center when it is fully induced [76,79,80]. It is therefore often used as an internal standard for the concentration of PSII and can be used for relative quantification of other free radical EPR signals from inside and outside of PSII. When PSII enriched membranes from *Arabidopsis* were illuminated at low temperatures a new radical signal emerged. The new signal is also located in the $g = 2$ region and is superimposed on the Y_D• signal (Fig. 4A, spectra a, dotted and dashed lines). Subtraction of Y_D• from the spectrum recorded after illumination revealed the formation of a symmetrical radical signal centered at $g = 2.0026$ with a line width of ~9 G (spectrum b, Table 2). This originates from oxidation of the accessory Chl_Z in PSII [78,81]. Illumination at 200 K or at 77 K induced the Chl_Z^+ radical in 27% or 30% of the PSII centers, respectively, estimated on the basis of Y_D• (Fig. 4A, spectrum b). We attribute the radical signal to the Chl_Z species rather than to the Car^+ radical (which is difficult to differentiate due to the similar g value and width) due to the fact that the induction of the Car^+ radical in spinach has been reported to require illumination at much lower temperatures [78]. The induction of the Chl_Z^+ radical (27%) after 200 K illumination is unusually high and indicates a substantial involvement of auxiliary donors in PSII from *Arabidopsis* at this temperature.

Cyt b_{559}, another component of the secondary electron transfer pathway in PSII, is known to undergo both photooxidation and photoreduction at special conditions [77]. The redox potential of Cyt b_{559} is variable, ranging from −50 to +450 mV depending on the activity status of PSII [77,82]. The redox forms and the amount of oxidized Cyt b_{559} can be studied by EPR spectroscopy, in particular in the g_z region of the EPR spectrum [77,83,84]. The g_z value depends on the redox potential form of Cyt b_{559}, and varies from $g = 2.92$ (the LP form) to $g = 3.10$ (the HP form) depending on species, preparation type, and the condition of PSII (Table 2) [23,77,84–86].

In Fig. 4B, the g_z peak of Cyt b_{559} from *Arabidopsis* is shown. Spectra were acquired from dark adapted PSII membranes (solid line) and after illumination at 77 K (dashed line). The spectrum from the dark adapted PSII showed an EPR signal with a peak at $g = 2.94$ which is

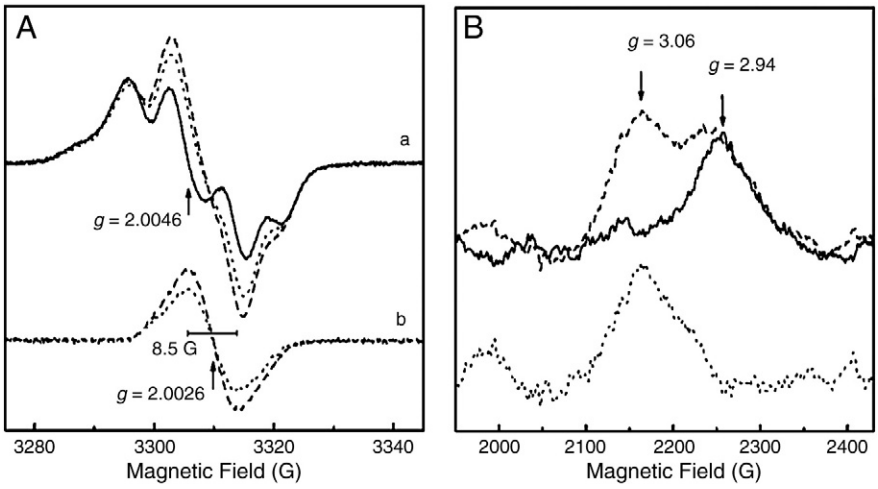

Fig. 4. (A) The effect of low temperature illumination on the radical EPR signals in the $g = 2$ region in PSII enriched membranes from *Arabidopsis*. Spectrum a was obtained from the dark-adapted membranes (solid line), after illumination at 200 K (dotted line) or 77 K (dashed line). Spectrum b shows the light minus dark difference spectrum after illumination at 200 K and 77 K. The bar in spectra a indicates $g = 2.0046$ and the bar in spectrum b indicates $g = 2.0024$. EPR conditions: microwave power 1.3 μW, microwave frequency 9.275 GHz, modulation amplitude 3.5 G, temperature 15 K. (B) EPR spectra from the g_z region of Cyt b_{559} recorded in dark adapted PSII membranes (solid line) and after 6 min illumination at 77 K (dashed line). The lower spectrum is the light minus dark difference spectrum (dotted line). EPR conditions: microwave power 5 mW, microwave frequency 9.275 GHz, modulation amplitude 15 G, temperature 15 K.

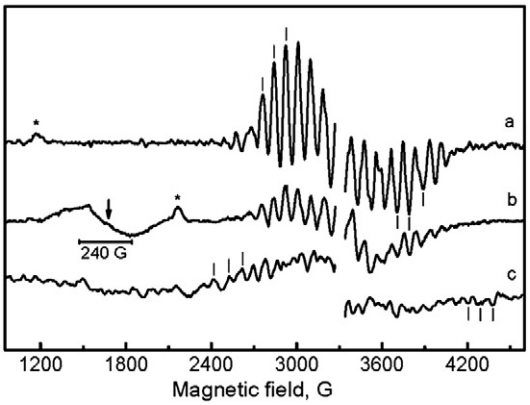

Fig. 5. The multiline signals from the $CaMn_4O_x$-cluster in PSII membranes from *Arabidopsis*. Spectra a and b show light minus dark difference spectra from the S_2-state obtained after a single laser flash in the presence of 0.5 mM PpBQ and 3% (v/v) methanol (a) or after 6 min continuous illumination at 200 K in the absence of the external electron acceptor and methanol (b). The arrow in b indicates the formation of the $g=4.1$ signal from the S_2-state. Spectrum c shows the light minus dark difference spectrum from the S_0-state obtained after three laser flashes in the presence of 0.5 mM P*p*BQ and 3% (v/v) methanol. Spectrum c was obtained by subtraction of 10% of the S_2 multiline signal (from spectra a) from the original spectrum. This subtraction was necessary to remove the contribution from the 10% of PSII centers that remained in the S_2-state after the 3 flashes. Bars in spectra a and c indicate peaks used for signal quantification. Asterisks show oxidation of the non-heme iron (spectrum a) and Cyt b_{559} (spectrum b). The region around $g=2$ is omitted for clarity. EPR conditions: microwave power 10 mW (spectra a and b) or 20 mW (spectrum c), microwave frequency 9.275 GHz, modulation amplitude 20 G, temperature 7 K.

attributed to the oxidized low potential (LP) form of Cyt b_{559} ([77,82], and references therein). Illumination at 77 K results in formation of a new peak at $g=3.06$ due to oxidation of the previously reduced high potential (HP) form. This is also shown as the light minus dark difference spectrum (Fig. 4B, dotted line). Integration of the spectra revealed that 40% of the total amount of Cyt b_{559} exists in the LP form and 60% in the HP form. This is similar to the results obtained from spinach PSII membranes in our preparation [84].

It is notable that illumination at 77 K resulted in oxidation of 30% of Chl_Z (Fig. 4A) and 60% of Cyt b_{559} (Fig. 4B). Thus we conclude that the absolute majority (probably all) of PSII centers (90%) in our preparation from *Arabidopsis* carry out efficient charge separation and electron transfer in the auxiliary pathway at this temperature.

3.2.1. EPR signals originating from the donor side of PSII — S_2-state and S_0-state multiline signals

Fig. 5 shows the EPR spectra from the S_2-state and the S_0-state recorded in PSII enriched membranes from *Arabidopsis* (see also Table 2). Spectra a and c were recorded after one flash (i.e. predominantly from the S_2-state) and three flashes (i.e. dominated by the S_0-state) respectively in the presence of 3% methanol (v/v) and P*p*BQ. Spectrum b was recorded after 6 min illumination at 200 K from PSII samples in the absence of methanol and an artificial electron acceptor. The S_2-state multiline signal from the $CaMn_4O_x$-cluster in PSII is centered around $g=2$ and exhibits at least 18 well resolved lines spaced by 80–90 G, spread over roughly 1800 G (Fig. 5, spectra a and b, Table 2) [87–89]. Our multiline signal obtained from *Arabidopsis* is similar to multiline signals reported from spinach [87,90,91], green algae [44] and cyanobacterial preparations [60,92,93]. In addition to the multiline signal, illumination at 200 K also produced the $g=4.1$ signal (Fig. 5, spectrum b). The signal at $g=4.1$ has an isotropic appearance with a line width of 240 G and no resolved hyperfine structure (Table 2) [88,89]. It is believed to originate from the excited $S=5/2$ state of the $CaMn_4O_x$-cluster [94,95]. The $g=4.1$ signal from PSII membranes of *Arabidopsis* resembles the signal reported earlier from spinach PSII preparations [88,89].

Similar to the situation in spinach, the S_2-state EPR signals from *Arabidopsis* are sensitive to methanol [96]. The addition of methanol completely eliminated the $g=4.1$ signal and enhanced the amplitude of the multiline signal (Fig. 5, compare spectra a and b). The S_2-state multiline signal, obtained in the presence of methanol and PpBQ, was found to be 3–4 times higher in amplitude if compared to the multiline signal obtained after 200 K illumination (Fig. 5, spectra a and b). It should be noted that illumination at 200 K induced not only multiline and the $g=4.1$ signals but also about 30% of the Chl_Z^+ radical and significant Cyt b_{559} oxidation (see spectrum b).

Another S-state dependent multiline EPR signal from the $CaMn_4O_x$-cluster can also be studied in the presence of methanol. This signal originates from the S_0-state and is spread over 2200 G around $g=2$ (Table 2) with different peak intensity and separation than the S_2-state multiline signal. The signal has been reported from spinach and cyanobacteria [45,97–99]. Fig. 5 (spectrum c) shows the S_0-state multiline signal obtained after 3 flashes in *Arabidopsis*. The spectrum shown was obtained by subtraction of 10% of the S_2-state multiline signal from the original EPR spectrum to eliminate contribution from the ca 10% remaining S_2-state PSII centers after the 3 flashes [99]. The deconvoluted S_0-state multiline signal exhibited narrower splitting between the peaks than the S_2 multiline signal (spectra a and b) and was more than 2000 G wide (Fig. 5, spectrum c, Table 2). The spectrum was quite stable in the dark and it showed no significant decay over 30 min incubation in the dark at room temperature. These properties are similar to those reported earlier in spinach and cyanobacteria [45,98].

3.2.2. EPR signals originating from the donor side of PSII — Y_z oxidation at cryogenic temperatures

Unlike the Y_D• radical, Y_Z• which is oxidized in the nanosecond to microsecond time range by P_{680}^+, normally decays in the submillisecond time range [100] due to reduction from the $CaMn_4O_x$-cluster. Y_Z• is not trivial to detect by conventional EPR techniques. However, at low temperatures, where the S state transitions are blocked, any formed Y_Z• can only decay by recombination with the acceptor side of PSII (with Q_A^-) which makes the live time of Y_Z• much longer and thus, possible for measurement [101–103]. Moreover, at cryogenic temperatures, the Y_Z radical interacts magnetically with the $CaMn_4O_x$-cluster. This results in S state specific broadening of the Y_Z• EPR signal and formation of so-called split EPR signals. Split EPR signals from all S states of the WOC (except the transient S_4-state), induced by illumination at liquid He temperature, have been reported from spinach or cyanobacteria [54,101,103–107]. These split EPR signals are useful probes to both S state turnover and the function of Y_Z [54,108].

Fig. 6 displays (see also Table 2) split EPR signals from the S_1-, S_2-, S_3- and S_0-states of WOC obtained from the PSII enriched membranes of *Arabidopsis* by illumination at 5 K. All signals presented are illumination minus dark subtracted spectra and exhibit a split part on the low and/or high field side of the $g=2$ region and a radical part at $g=2$.

Illumination with visible light induced both a fast decaying component ($t_{½}$ ca 3 min) and slower decaying components of the light induced EPR signals in agreement with earlier findings in spinach [101,107]. The slowly decaying component was present only in the radical part of the spectrum and has been shown to originate from oxidized Chl^+/Car^+ species in a fraction of the PSII centers. The oxidation of Chl/Car is associated with the secondary electron transfer pathway (see above) [107] and does not interfere with our analysis of the split EPR signals that originate from the WOC. In contrast, the fast decaying components of the light induced spectra represent the split signals in the different S states and the decay reflects recombination between Q_A^- and Y_Z• (see references [107,108] for a discussion of this phenomenon).

The Split S_1 EPR spectrum induced with visible light at 5 K in *Arabidopsis* is shown in Fig. 6A. The spectrum exhibits a characteristic single peak at $g=2.035$ (Table 2) identical in position to the Split S_1 signal from spinach or cyanobacteria [54,55,101,103,109–111].

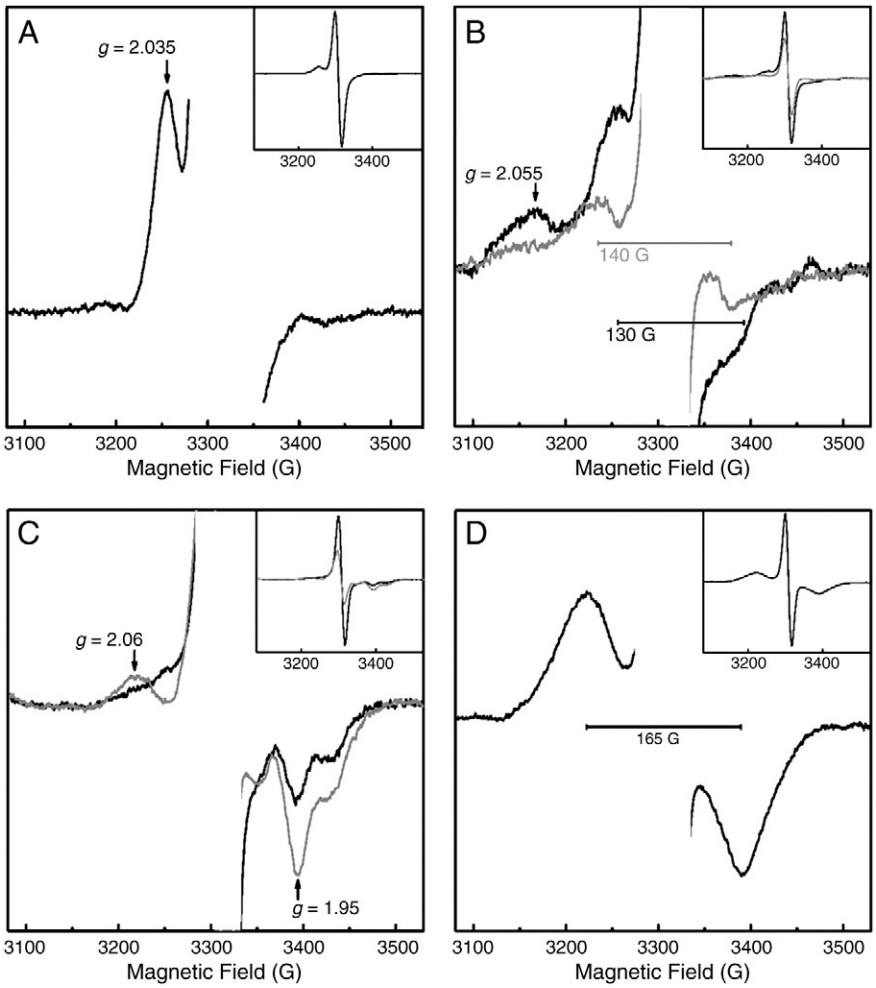

Fig. 6. Induction of the metallo-radical (Y_Z•) split EPR signals in different S states of the WOC in *Arabidopsis* by continuous white light illumination for 30 s at 5 K. The spectra shown are the difference spectra between spectra recorded during illumination and spectra recorded before illumination from the PSII membranes poised in the S_1-state (Split S_1 signal, A), in the S_2-state (Split S_2 signal, B), in the S_3-state (Split S_3 signal, C) and in the S_0-state (Split S_0 signal, D). The spectra in grey color (B) were induced in the presence of 3% (v/v) methanol and (C) by illumination by NIR light at 830 nm for 20 min. The region around $g = 2$ is omitted for clarity. The insets show the entire spectra including the $g = 2$ region. EPR conditions: microwave power 20 mW or 50 mW (for Split S_2 only), microwave frequency 9.275 GHz, modulation amplitude 15 G, temperature 5 K.

The Split S_2 EPR signal was reported to be induced either in the presence of methanol at 10 K (note that the presence of methanol inhibits the Split S_1 and split S_3 signals and modifies the Split S_0 signal [55,112] or by illumination at higher temperatures (77–190 K) [55]. We were able to trap both of the Split S_2 signals in *Arabidopsis* as shown in Fig. 6B. Illumination at 200 K and continuous illumination during lowering the temperature to 5 K allowed us to trap a complicated interaction signal, different from that reported in spinach [55]. This signal consists of a symmetrical 130 G wide split feature and an additional peak at $g = 2.055$ (Fig. 6B, black line). The symmetrical part is wider than that reported in spinach PSII membranes (116 G) where the additional low field peak was not reported [55]. Illumination of the PSII samples in the presence of methanol (3% v/v) at 5 K induced a 140 G wide symmetrical split signal (Table 2) also with a possible low field peak (Fig. 6B, grey line). The symmetrical part now was found to be narrower than spinach signal (160 G in presence of methanol, [55]).

The Split S_3 signal is formed in PSII samples exposed to 2 flashes (dominated by the S_3-state) by illumination both with visible light [104,107] and near infrared light [104,113] at cryogenic temperatures. In contrast to the signal induced by visible light, the near infrared induced signal is very stable at 5 K and shows no observable decay for at least 30 min [104]. Fig. 6C displays the Split S_3 signals induced by visible light (black line) and 830 nm light (grey line) at 5 K in *Arabidopsis*. Both signals are very similar to the corresponding signals reported from spinach [107,109,113] and cyanobacteria [114]. The signal has a double trough at $g = 1.95$ and 1.93 position and a peak (for the near infrared induced signal) at $g = 2.06$ (Table 2). It is also clear that the central part of the signal induced by the near infrared light is smaller which reflects that it lacks any contributions from the Chl^+/Car^+ radicals (Fig. 6C, inset).

The light induced Split S_0 signal obtained from PSII membranes after 3 laser flashes (sample dominated by S_0-state) is shown in Fig. 6D. Illumination at 5 K gave rise to a broad symmetrical signal separated by 165 G (Table 2). The shape and size of this signal resemble the ca 160 G wide signal previously assigned to the S_0Y_Z• state in spinach [101] and cyanobacteria [114].

Thus, the split EPR signals from the WOC in *Arabidopsis* were induced with high yield and precision. Taken together with the multiline signals these EPR probes provide powerful tools to study the WOC in different mutants available in *Arabidopsis*.

4. Conclusions

A complete register of perpendicular mode X-band EPR signals from the donor and acceptor sides of PSII, as well as from the auxiliary electron donors, is reported from the PSII enriched membranes isolated from *Arabidopsis* plants. The EPR signals were obtained in high yield with precision, allowing also quantitative measurements. In

total, about 20 different EPR signals covering almost all of the electron transfer components in PSII were recorded. This study extends the comparison between plant species and opens a possibility to study PSII electron transfer reactions in the library of mutants available in *Arabidopsis*.

Acknowledgements

This work was supported by the Swedish Research Council, the Swedish Energy Agency and the Knut and Alice Wallenberg Foundation. EMA and YA acknowledge the financial support from the Academy of Finland (CoE project 118637). The authors also would like to thank Ms. Maija Holmstrom for excellent technical assistance.

References

[1] The Arabidopsis Genome Initiative, Analysis of the genome sequence of the flowering plant *Arabidopsis thaliana*, Nature 408 (2000) 796–815.
[2] D.W. Meinke, J.M. Cherry, C. Dean, S.D. Rounsley, M. Koornneef, *Arabidopsis thaliana*: a model plant for genome analysis, Science 282 (1998) 662–682.
[3] D. Leister, A. Schneider, W.J. Kwang, From gene to photosynthesis in *Arabidopsis thaliana*, in: W.J. Kwang (Ed.), International Review of Cytology, Academic Press, Amsterdam, 2003, pp. 31–83.
[4] L.A. Mueller, P. Zhang, S.Y. Rhee, AraCyc: a biochemical pathway database for *Arabidopsis*, Plant Physiol. 132 (2003) 453–460.
[5] K.K. Niyogi, A.R. Grossman, O. Bjorkman, *Arabidopsis* mutants define a central role for the xanthophyll cycle in the regulation of photosynthetic energy conversion, Plant Cell 10 (1998) 1121–1134.
[6] X.-P. Li, O. Bjorkman, C. Shih, A.R. Grossman, M. Rosenquist, S. Jansson, K.K. Niyogi, A pigment-binding protein essential for regulation of photosynthetic light harvesting, Nature 403 (2000) 391–395.
[7] J. Andersson, M. Wentworth, G. Walters Robin, A. Howard Caroline, V. Ruban Alexander, P. Horton, S. Jansson, Absence of the Lhcb1 and Lhcb2 proteins of the light-harvesting complex of photosystem II — effects on photosynthesis, grana stacking and fitness, Plant J. 35 (2003) 350–361.
[8] R. Gupta, Z. He, S. Luan, Functional relationship of cytochrome c_6 and plastocyanin in *Arabidopsis*, Nature 417 (2002) 567–571.
[9] Y. Munekage, M. Hashimoto, C. Miyake, K. Tomizawa, T. Endo, M. Tasaka, T. Shikanai, Cyclic electron flow around photosystem I is essential for photosynthesis, Nature 429 (2004) 579–582.
[10] M.K. Munshi, Y. Kobayashi, T. Shikanai, CHLORORESPIRATORY REDUCTION 6 is a novel factor required for accumulation of the chloroplast NAD(P)H dehydrogenase complex in *Arabidopsis*, Plant Physiol. 141 (2006) 737–744.
[11] L. Minna, A. Yagut, K. Heidi, P. Mirva, B. Natalia, S. Marjaana, R. Eevi, A.S. Tiina, A. Eva-Mari, M. Paula, Structural and functional characterization of ferredoxin-$NADP^+$-oxidoreductase using knock-out mutants of *Arabidopsis*, Plant J. 49 (2007) 1041–1052.
[12] L. Peng, Y. Fukao, M. Fujiwara, T. Takami, T. Shikanai, Efficient operation of NAD(P)H dehydrogenase requires supercomplex formation with photosystem I via minor LHCI in *Arabidopsis*, Plant Cell 21 (2009) 3623–3640.
[13] C. Lunde, P.E. Jensen, A. Haldrup, J. Knoetzel, H.V. Scheller, The PSI-H subunit of photosystem I is essential for state transitions in plant photosynthesis, Nature 408 (2000) 613–615.
[14] M. Yuri, T. Satomi, E. Tsuyoshi, J. Peter, H. Takashi, S. Toshiharu, Cytochrome b_6f mutation specifically affects thermal dissipation of absorbed light energy in *Arabidopsis*, Plant J. 28 (2001) 351–359.
[15] S. Bailey, P. Horton, R.G. Walters, Acclimation of *Arabidopsis thaliana* to the light environment: the relationship between photosynthetic function and chloroplast composition, Planta 218 (2004) 793–802.
[16] A. Zelisko, M. Garcia-Lorenzo, G. Jackowski, S. Jansson, C. Funk, AtFtsH6 is involved in the degradation of the light-harvesting complex II during high-light acclimation and senescence, Proc. Nat. Acad. Sci. U. S. A. 102 (2005) 13699–13704.
[17] T. Mikko, P. Mirva, S. Marjaana, S. Sari, M. Paula, V. Julia, V. Alexander, A. Yagut, A. Eva-Mari, State transitions revisited—a buffering system for dynamic low light acclimation of *Arabidopsis*, Plant Mol. Biol. 62 (2006) 779–793.
[18] P.J. Matthew, V.R. Alexander, Arabidopsis plants lacking PsbS protein possess photoprotective energy dissipation, Plant J. 61 (2010) 283–289.
[19] V. Fey, R. Wagner, K. Bräutigam, M. Wirtz, R. Hell, A. Dietzmann, D. Leister, R. Oelmüller, T. Pfannschmidt, Retrograde plastid redox signals in the expression of nuclear genes for chloroplast proteins of *Arabidopsis thaliana*, J. Biol. Chem. 280 (2005) 5318–5328.
[20] S. Nilsson Cederholm, H. Bäckman, P. Pesaresi, D. Leister, E. Glaser, Deletion of an organellar peptidasome PreP affects early development in *Arabidopsis thaliana*, Plant Mol. Biol. 71 (2009) 497–508.
[21] F. Mamedov, H. Stefansson, P.-Å. Albertsson, S. Styring, Photosystem II in different parts of the thylakoid membrane: a functional comparison between different domains, Biochemistry 39 (2000) 10478–10486.
[22] J.P. Dekker, E.J. Boekema, Supramolecular organization of thylakoid membrane proteins in green plants, Biochim. Biophys. Acta 1706 (2005) 12–39.
[23] F. Mamedov, R. Danielsson, R. Gadjieva, P.-Å. Albertsson, S. Styring, EPR characterization of photosystem II from different domains of the thylakoid membrane, Biochemistry 47 (2008) 3883–3891.
[24] J. Barber, Photosystem II: the engine of life, Q. Rev. Biophys. 36 (2003) 71–89.
[25] N. Nelson, C.F. Yocum, Structure and function of photosystems I and II, Annu. Rev. Plant Biol. 57 (2006) 521–565.
[26] G. Renger, Photosynthetic water oxidation to molecular oxygen: apparatus and mechanism, Biochim. Biophys. Acta 1503 (2001) 210–228.
[27] C. Goussias, A. Boussac, A.W. Rutherford, Photosystem II and photosynthetic oxidation of water: an overview, Philos. Trans. R. Soc. Lond. B 357 (2002) 1369–1381.
[28] K.N. Ferreira, T.M. Iverson, K. Maghlaoui, J. Barber, S. Iwata, Architecture of the photosynthetic oxygen-evolving center, Science 303 (2004) 1831–1838.
[29] B. Loll, J. Kern, W. Saenger, A. Zouni, J. Biesiadka, Towards complete cofactor arrangement in the 3.0 Å resolution structure of photosystem II, Nature 438 (2005) 1040–1044.
[30] J.P. McEvoy, G.W. Brudvig, Water-splitting chemistry of photosystem II, Chem. Rev. 106 (2006) 4455–4483.
[31] B. Kok, B. Forbush, M. McGloin, Cooperation of charges in photosynthetic O_2 evolution—I. A linear four step mechanism, Photochem. Photobiol. 11 (1970) 457–475.
[32] L.-X. Shi, Z.J. Lorkovic, R. Oelmuller, W.P. Schröder, The low molecular mass PsbW protein is involved in the stabilization of the dimeric photosystem II complex in *Arabidopsis thaliana*, J. Biol. Chem. 275 (2000) 37945–37950.
[33] Y. Allahverdiyeva, F. Mamedov, M. Suorsa, S. Styring, I. Vass, E.-M. Aro, Insights into the function of PsbR protein in *Arabidopsis thaliana*, Biochim. Biophys. Acta 1767 (2007) 677–685.
[34] X. Yi, S.R. Hargett, H. Liu, L.K. Frankel, T.M. Bricker, The PsbP protein is required for photosystem II complex assembly/stability and photoautotrophy in *Arabidopsis thaliana*, J. Biol. Chem. 282 (2007) 24833–24841.
[35] H. Liu, L.K. Frankel, T.M. Bricker, Functional analysis of photosystem II in a PsbO-1-deficient mutant in *Arabidopsis thaliana*, Biochemistry 46 (2007) 7607–7613.
[36] S. Sirpiö, Y. Allahverdiyeva, M. Suorsa, V. Paakkarinen, J. Vainonen, N. Battchikova, E.-M. Aro, TLP18.3, a novel thylakoid lumen protein regulating photosystem II repair cycle, Biochem. J. 406 (2007) 415–425.
[37] S. Sirpiö, A. Khrouchtchova, Y. Allahverdiyeva, M. Hansson, R. Fristedt, A.V. Vener, H.V. Scheller, P.E. Jensen, A. Haldrup, E.-M. Aro, AtCYP38 ensures early biogenesis, correct assembly and sustenance of photosystem II, Plant J. 55 (2008) 639–651.
[38] Y. Allahverdiyeva, F. Mamedov, M. Holmström, M. Nurmi, B. Lundin, S. Styring, C. Spetea, E.-M. Aro, Comparison of the electron transport properties of the *psbo1* and *psbo2* mutants of *Arabidopsis thaliana*, Biochim. Biophys. Acta 1787 (2009) 1230–1237.
[39] D.A. Berthold, G.T. Babcock, C.F. Yocum, A highly resolved, oxygen-evolving photosystem II preparation from spinach thylakoid membranes: EPR and electron-transport properties, FEBS Lett. 134 (1981) 231–234.
[40] R.J. Porra, W.A. Thompson, P.E. Kriedemann, Determination of accurate extinction coefficients and simultaneous equations for assaying chlorophylls *a* and *b* extracted with four different solvents: verification of the concentration of chlorophyll standards by atomic absorption spectroscopy, Biochim. Biophys. Acta 975 (1989) 384–394.
[41] U.K. Laemmli, Cleavage of structural proteins during the assembly of the head of bacteriophage T4, Nature 227 (1970) 680–685.
[42] R. Danielsson, P.-Å. Albertsson, F. Mamedov, S. Styring, Quantification of photosystem I and II in different parts of the thylakoid membrane from spinach, Biochim. Biophys. Acta 1608 (2004) 53–61.
[43] S. Styring, A.W. Rutherford, In the oxygen-evolving complex of photosystem II the S_0 state is oxidized to the S_1 state by D^+ (signal II_{slow}), Biochemistry 26 (1987) 2401–2405.
[44] S. Styring, A.W. Rutherford, Deactivation kinetics and temperature dependence of the S-state transitions in the oxygen-evolving system of photosystem II measured by EPR spectroscopy, Biochim. Biophys. Acta 933 (1988) 378–387.
[45] K.A. Åhrling, S. Peterson, S. Styring, An oscillating manganese electron paramagnetic resonance signal from the S_0 state of the oxygen evolving complex in photosystem II, Biochemistry 36 (1997) 13148–13152.
[46] F.M. Ho, S.F. Morvaridi, F. Mamedov, S. Styring, Enhancement of Y_D• spin relaxation by the $CaMn_4$ cluster in photosystem II detected at room temperature: a new probe for the S-cycle, Biochim. Biophys. Acta 1767 (2007) 5–14.
[47] A.W. Rutherford, J.L. Zimmermann, A new EPR signal attributed to the primary plastosemiquinone acceptor in photosystem II, Biochim. Biophys. Acta 767 (1984) 168–175.
[48] W.F.J. Vermaas, A.W. Rutherford, EPR measurements on the effects of bicarbonate and triazine resistance on the acceptor side of photosystem II, FEBS Lett. 175 (1984) 243–248.
[49] S. Styring, I. Virgin, A. Ehrenberg, B. Andersson, Strong light photoinhibition of electrontransport in Photosystem II. Impairment of the function of the first quinone acceptor, Q_A, Biochim. Biophys. Acta 1015 (1990) 269–278.
[50] A.F. Miller, G.W. Brudvig, A guide to electron paramagnetic resonance spectroscopy of photosystem II membranes, Biochim. Biophys. Acta 1056 (1991) 1–18.
[51] V.V. Klimov, E. Dolan, E.R. Shaw, B. Ke, Interaction between the intermediary electron acceptor (pheophytin) and a possible plastoquinone–iron complex in photosystem II reaction centers, Proc. Nat. Acad. Sci. U. S. A. 77 (1980) 7227–7231.
[52] V.V. Klimov, E. Dolan, B. Ke, EPR properties of an intermediary electron acceptor (pheophytin) in photosystem-II reaction centers at cryogenic temperatures, FEBS Lett. 112 (1980) 97–100.
[53] I. Vass, S. Styring, Spectroscopic characterization of triplet forming states in photosystem II, Biochemistry 31 (1992) 5957–5963.

[54] G. Han, F.M. Ho, K.G.V. Havelius, S.F. Morvaridi, F. Mamedov, S. Styring, Direct quantification of the four individual S states in photosystem II using EPR spectroscopy, Biochim. Biophys. Acta 1777 (2008) 496–503.

[55] N. Ioannidis, G. Zahariou, V. Petrouleas, Trapping of the S_2 to S_3 state intermediate of the oxygen-evolving complex of photosystem II, Biochemistry 45 (2006) 6252–6259.

[56] G. Bernat, F. Morvaridi, Y. Feyziyev, S. Styring, pH dependence of the four individual transitions in the catalytic S-cycle during photosynthetic oxygen evolution, Biochemistry 41 (2002) 5830–5843.

[57] H. Dau, Molecular mechanisms and quantitative models of variable photosystem II fluorescence, Photochem. Photobiol. 60 (1994) 1–23.

[58] J.H.A. Nugent, B.A. Diner, M.C.W. Evans, Direct detection of the electron acceptor of photosystem II: evidence that Q is an iron–quinone complex, FEBS Lett. 124 (1981) 241–244.

[59] A.W. Rutherford, P. Mathis, A relationship between the midpoint potential of the primary acceptor and low temperature photochemistry in photosystem II, FEBS Lett. 154 (1983) 328–334.

[60] F. Mamedov, M.M. Nowaczyk, A. Thapper, M. Rögner, S. Styring, Functional characterization of monomeric photosystem II core preparations from *Thermosynechococcus elongatus* with or without the Psb27 protein, Biochemistry 46 (2007) 5542–5551.

[61] V. Petrouleas, A.R. Crofts, The iron–quinone accepter complex, in: T.J. Wydrzynski, K. Satoh (Eds.), Photosystem II — The Light-Driven Water: Plastoquinone Oxidoreductase, Springer, The Netherlands, 2005, pp. 177–206.

[62] J.L. Zimmermann, A.W. Rutherford, Photoreductant-induced oxidation of Fe^{2+} in the electron-acceptor complex of photosystem II, Biochim. Biophys. Acta 851 (1986) 416–423.

[63] V. Petrouleas, B.A. Diner, Light-induced oxidation of the acceptor-side Fe(II) of photosystem II by exogenous quinones acting through the Q_B binding site. I. Quinones, kinetics and pH-dependence, Biochim. Biophys. Acta 893 (1987) 126–137.

[64] B.A. Diner, V. Petrouleas, Q_{400}, the non-heme iron of the photosystem II iron–quinone complex. A spectroscopic probe of quinone and inhibitor binding to the reaction center, Biochim. Biophys. Acta 895 (1987) 107–125.

[65] R. Aasa, L.-E. Andreasson, S. Styring, T. Vänngård, The nature of the Fe(III) EPR signal from the acceptor-side iron in photosystem II, FEBS Lett. 243 (1989) 156–160.

[66] V. Petrouleas, B.A. Diner, Identification of Q_{400}, a high-potential electron acceptor of photosystem II, with the iron of the quinone–iron acceptor complex, Biochim. Biophys. Acta 849 (1986) 264–275.

[67] H.A. Frank, Ö. Hansson, P. Mathis, EPR and optical changes of the photosystem II reaction center produced by low temperature illumination, Photosynth. Res. 20 (1989) 279–289.

[68] J.H.A. Nugent, A. Telfer, C. Demetriou, J. Barber, Electron transfer in the isolated photosystem II reaction centre complex, FEBS Lett. 255 (1989) 53–58.

[69] A.W. Rutherford, D.R. Paterson, J.E. Mullet, A light-induced spin-polarized triplet detected by EPR in photosystem II reaction centers, Biochim. Biophys. Acta 635 (1981) 205–214.

[70] A.W. Rutherford, J.E. Mullet, Reaction center triplet states in photosystem I and photosystem II, Biochim. Biophys. Acta 635 (1981) 225–235.

[71] F.J.E.v. Mieghem, W. Nitschke, P. Mathis, A.W. Rutherford, The influence of the quinone–iron electron acceptor complex on the reaction centre photochemistry of photosystem II, Biochim. Biophys. Acta 977 (1989) 207–214.

[72] A.W. Rutherford, How close is the analogy between the reaction center of photosystem-II and that of purple bacteria, Biochem. Soc. Trans. 14 (1986) 15–17.

[73] I. Vass, S. Styring, T. Hundal, A. Koivuniemi, E. Aro, B. Andersson, Reversible and irreversible intermediates during photoinhibition of photosystem II: stable reduced Q_A species promote chlorophyll triplet formation, Proc. Nat. Acad. Sci. U. S. A. 89 (1992) 1408–1412.

[74] A. Magnuson, M. Rova, F. Mamedov, P.-O. Fredriksson, S. Styring, The role of cytochrome b_{559} and tyrosine$_D$ in protection against photoinhibition during in vivo photoactivation of photosystem II, Biochim. Biophys. Acta 1411 (1999) 180–191.

[75] J.C. De Paula, J.B. Innes, G.W. Brudvig, Electron transfer in photosystem II at cryogenic temperatures, Biochemistry 24 (1985) 8114–8120.

[76] B.A. Barry, G.T. Babcock, Tyrosine radicals are involved in the photosynthetic oxygen-evolving system, Proc. Nat. Acad. Sci. U. S. A. 84 (1987) 7099–7103.

[77] D.H. Stewart, G.W. Brudvig, Cytochrome b_{559} of photosystem II, Biochim. Biophys. Acta 1367 (1998) 63–87.

[78] J. Hanley, Y. Deligiannakis, A. Pascal, P. Faller, A.W. Rutherford, Carotenoid oxidation in photosystem II, Biochemistry 38 (1999) 8189–8195.

[79] B. Commoner, J.J. Heise, J. Townsend, Light-induced paramagnetism in chloroplasts, Proc. Natl. Acad. Sci. U. S. A. 42 (1956) 710–718.

[80] G.T. Babcock, K. Sauer, Electron paramagnetic resonance signal II in spinach chloroplasts. I. Kinetic analysis for untreated chloroplasts, Biochim. Biophys. Acta (BBA) — Bioenerg. 325 (1973) 483–503.

[81] R. Malkin, A.J. Bearden, Detection of a free radical in the primary reaction of chloroplast photosystem II, Proc. Nat. Acad. Sci. U. S. A. 70 (1973) 294–297.

[82] O. Kaminskaya, V.A. Shuvalov, G. Renger, Evidence for a novel quinone-binding site in the photosystem II (PS II) complex that regulates the redox potential of cytochrome b_{559}, Biochemistry 46 (2007) 1091–1105.

[83] F.A. Walker, H. Boi Hanh, W.R. Scheidt, S.R. Osvath, Models of the cytochromes *b*. Effect of axial ligand plane orientation on the EPR and Moessbauer spectra of low-spin ferrihemes, J. Am. Chem. Soc. 108 (1986) 5288–5297.

[84] L.K. Thompson, A.F. Miller, C.A. Buser, J.C. De Paula, G.W. Brudvig, Characterization of the multiple forms of cytochrome b_{559} in photosystem II, Biochemistry 28 (1989) 8048–8056.

[85] G.T. Babcock, W.R. Widger, W.A. Cramer, W.A. Oertling, J.G. Metz, Axial ligands of chloroplast cytochrome *b*-559: identification and requirement for a heme-crosslinked polypeptide structure, Biochemistry 24 (1985) 3638–3645.

[86] C. Berthomieu, A. Boussac, W. Maentele, J. Breton, E. Nabedryk, Molecular changes following oxidoreduction of cytochrome b_{559} characterized by Fourier transform infrared difference spectroscopy and electron paramagnetic resonance: photooxidation in photosystem II and electrochemistry of isolated cytochrome b_{559} and iron protoporphyrin IX-bisimidazole model compounds, Biochemistry 31 (1992) 11460–11471.

[87] G.C. Dismukes, Y. Siderer, EPR spectroscopic observations of a manganese center associated with water oxidation in spinach chloroplasts, FEBS Lett. 121 (1980) 78–80.

[88] J.L. Casey, K. Sauer, EPR detection of a cryogenically photogenerated intermediate in photosynthetic oxygen evolution, Biochim. Biophys. Acta 767 (1984) 21–28.

[89] J.L. Zimmermann, A.W. Rutherford, EPR studies of the oxygen-evolving enzyme of photosystem II, Biochim. Biophys. Acta 767 (1984) 160–167.

[90] G.C. Dismukes, Y. Siderer, Intermediates of a polynuclear manganese center involved in photosynthetic oxidation of water, Proc. Nat. Acad. Sci. U. S. A. 78 (1981) 274–278.

[91] J.L. Zimmermann, A.W. Rutherford, Electron paramagnetic resonance properties of the S_2 state of the oxygen-evolving complex of photosystem II, Biochemistry 25 (1986) 4609–4615.

[92] A.E. McDermott, V.K. Yachandra, R.D. Guiles, J.L. Cole, S.L. Dexheimer, R.D. Britt, K. Sauer, M.P. Klein, Characterization of the manganese oxygen-evolving complex and the iron–quinone acceptor complex in photosystem II from a thermophilic cyanobacterium by electron paramagnetic resonance and X-ray absorption spectroscopy, Biochemistry 27 (1988) 4021–4031.

[93] D.L. Kirilovsky, A.G.P. Boussac, F.J.E. Van Mieghem, J.M.R.C. Ducruet, P.R. Setif, J. Yu, W.F.J. Vermaas, A.W. Rutherford, Oxygen-evolving photosystem II preparation from wild-type and photosystem II mutants of *Synechocystis* Sp. PCC 6803, Biochemistry 31 (1992) 2099–2107.

[94] A. Haddy, W.R. Dunham, R.H. Sands, R. Aasa, Multifrequency EPR investigations into the origin of the S_2-state signal at $g = 4$ of the O_2-evolving complex, Biochim. Biophys. Acta 1099 (1992) 25–34.

[95] A. Haddy, K.V. Lakshmi, G.W. Brudvig, H.A. Frank, Q-band EPR of the S_2 state of photosystem II confirms an $S = 5/2$ origin of the X-band $g = 4.1$ signal, Biophys. J. 87 (2004) 2885–2896.

[96] R.J. Pace, P. Smith, R. Bramley, D. Stehlik, EPR saturation and temperature dependence studies on signals from the oxygen-evolving centre of photosystem II, Biochim. Biophys. Acta 1058 (1991) 161–170.

[97] J. Messinger, J.H. Nugent, M.C. Evans, Detection of an EPR multiline signal for the S_0^- state in photosystem II, Biochemistry 36 (1997) 11055–11060.

[98] J. Messinger, J.H. Robblee, W.O. Yu, K. Sauer, V.K. Yachandra, M.P. Klein, The S_0 state of the oxygen-evolving complex in photosystem II is paramagnetic: detection of an EPR multiline signal, J. Am. Chem. Soc. 119 (1997) 11349–11350.

[99] K.A. Åhrling, S. Peterson, S. Styring, The S_0 state EPR signal from the Mn cluster in photosystem II arises from an isolated $S = 1/2$ ground state, Biochemistry 37 (1998) 8115–8120.

[100] G. Renger, Coupling of electron and proton transfer in oxidative water cleavage in photosynthesis, Biochim. Biophys. Acta 1655 (2004) 195–204.

[101] C. Zhang, S. Styring, Formation of split electron paramagnetic resonance signals in photosystem II suggests that tyrosine$_Z$ can be photooxidized at 5 K in the S_0 and S_1 states of the oxygen-evolving complex, Biochemistry 42 (2003) 8066–8076.

[102] D. Koulougliotis, C. Teutloff, Y. Sanakis, W. Lubitz, V. Petrouleas, The S_1Y_Z• metalloradical intermediate in photosystem II: an X- and W-band EPR study, Phys. Chem. Chem. Phys. 6 (2004) 4859–4863.

[103] C. Zhang, A. Boussac, A.W. Rutherford, Low-temperature electron transfer in photosystem II: a tyrosyl radical and semiquinone charge pair, Biochemistry 43 (2004) 13787–13795.

[104] N. Ioannidis, J.H.A. Nugent, V. Petrouleas, Intermediates of the S_3 state of the oxygen-evolving complex of photosystem II, Biochemistry 41 (2002) 9589–9600.

[105] J.H.A. Nugent, I.P. Muhiuddin, M.C.W. Evans, Electron transfer from the water oxidizing complex at cryogenic temperatures: the S_1 to S_2 step, Biochemistry 41 (2002) 4117–4126.

[106] V. Petrouleas, D. Koulougliotis, N. Ioannidis, Trapping of metalloradical intermediates of the S-states at liquid helium temperatures. Overview of the phenomenology and mechanistic implications, Biochemistry 44 (2005) 6723–6728.

[107] K.G.V. Havelius, J.-H. Su, Y. Feyziyev, F. Mamedov, S. Styring, Spectral resolution of the split EPR signals induced by illumination at 5 K from the S_1, S_3, and S_0 states in photosystem II, Biochemistry 45 (2006) 9279–9290.

[108] K.G.V. Havelius, J. Sjoholm, F.M. Ho, F. Mamedov, S. Styring, Metalloradical EPR signals from the YZ·S-state intermediates in photosystem II Appl, Magn. Reson. 37 (2010) 151–176.

[109] J.-H. Su, K.G.V. Havelius, F. Mamedov, F.M. Ho, S. Styring, Split EPR signals from photosystem II are modified by methanol, reflecting S state-dependent binding and alterations in the magnetic coupling in the $CaMn_4$ cluster, Biochemistry 45 (2006) 7617–7627.

[110] K.G.V. Havelius, S. Styring, pH dependent competition between Y_Z and Y_D in photosystem II probed by illumination at 5 K, Biochemistry 46 (2007) 7865–7874.

[111] J.-H. Su, K.G.V. Havelius, F.M. Ho, G. Han, F. Mamedov, S. Styring, Formation spectra of the EPR split signals from the S_0, S_1, and S_3 states in photosystem II induced by monochromatic light at 5 K, Biochemistry 46 (2007) 10703–10712.
[112] N. Ioannidis, G. Zahariou, V. Petrouleas, The EPR spectrum of tyrosine $Z^{\bullet}$ and its decay kinetics in O_2-evolving photosystem II preparations, Biochemistry 47 (2008) 6292–6300.
[113] N. Ioannidis, V. Petrouleas, Electron paramagnetic resonance signals from the S_3 state of the oxygen-evolving complex. A broadened radical signal induced by low-temperature near-infrared light illumination, Biochemistry 39 (2000) 5246–5254.
[114] A. Boussac, M. Sugiura, T.L. Lai, A.W. Rutherford, Low-temperature photochemistry in photosystem II from *Thermosynechococcus elongatus* induced by visible and near-infrared light, Philos. Trans. R. Soc. B Biol. Sci. 363 (2008) 1203–1210.